Cement and Concrete Composites 72 (2016) 257–267

Contents lists available at ScienceDirect

Cement and Concrete Composites

journal homepage: www.elsevier.com/locate/cemconcomp

Predictive convection zone depth of chloride in concrete under chloride environment

Peng Liu [a, b], Zhiwu Yu [a, b, *], Zhaohui Lu [a, b], Ying Chen [a, b], Xiaojie Liu [a, b]

[a] School of Civil Engineering, Central South University, 22 Shaoshan Road, Changsha 410075, China
[b] National Engineering Laboratory for High Speed Railway Construction, Central South University, Changsha 410075, China

ARTICLE INFO

Article history:
Received 20 November 2015
Received in revised form
7 June 2016
Accepted 20 June 2016
Available online 21 June 2016

Keywords:
Concrete
Chloride ion
Concentration
Convection zone depth
Water influential depth

ABSTRACT

Based on the assumption that chloride concentration and water influential depth change linearly in convective zone, the chloride convection zone depth is used in Fick's diffusion law to investigate the chloride diffusion characteristic of concrete at tidal zones. In this study, an artificial simulation environment and field tests were carried out to validate and calibrate the rationality of the chloride convection zone depth model. The distribution model of surface chloride concentration in concrete was determined by exploring the correlations among chloride concentration, elevation, time and linear distance from seaside. The results illustrated that the depth of chloride convection zone on the concrete surface varied and manifested in terms of a function of water influential depth. The relation between the surface chloride concentration and the linear distance from the seaside followed an S-curve function equation. The similarities and differences regarding the characteristic of chloride diffusion in concrete between experimental and in-situ test were discussed for surface chloride concentration, chloride convection zone depth and chloride diffusion coefficient.

1. Introduction

Deterioration of reinforced concrete (RC) is a major problem for construction engineering (e.g. bridges, harbours and off-shore platforms) in marine environments, and thus chloride ingress is the main factor affecting the durability of RC structures [1–3]. Most of previous studies [4–7] on the chloride diffusion characteristic in RC are based on Fick's second law of diffusion. Under alternating wetting and drying cycles in practice, the depth of chloride convection zone is considered as a key variable in Fick's second law. Numerous values of chloride convection zone depths have been recommended, e.g., depth of 14 mm for marine concretes [8] and a range from 20 mm to 30 mm by Rincon et al. [9]. Ye et al. [10] proposed a convection zone depth ranging from 5 mm to 15 mm for sound concrete. While for the cracked zone depth, a range from approximately 20 mm–35 mm was estimated based on experimental results. Lei et al. [11] suggested that the corresponding convection zone depth for the segment structure of a shield tunnel should be usually set as 5 mm. Cui et al. [12] found that the depth of convection zones increased with increasing crack width. When the crack width was less than 0.3 mm, the depth ranged from 10 mm to 15 mm. For cracks larger than 0.3 mm, the corresponding depth reached 15 mm–20 mm. Li et al. [13] analytically treated the water influential depth as the convection zone depth. Castro et al. [14] proposed that there was a continuous dampened zone close to the concrete nucleus, and wet and dry zones formed on the surface. However, the available research results above on chloride convection zone depth are most based on measured data which lacks the support of theoretical analyses. Therefore, an effective prediction models is needed for estimating the depth of chlorlide convection zone.

Given that fixed values of depth of chloride convection zones lead to considerable uncertainties in the model outputs (e.g. the time to corrosion initiation), theoretical analyses of chloride concentration profiles may result in serious consequences (e.g. the real service life, the optimal time for inspection and maintenance), and thus analytical results fail to reflect the real deterioration of RC under chloride environments. Therefore, the depth of chloride convective zones recommended in Refs. [8–13] cannot be directly applied to different RC and environmental conditions. Actually, chloride convection zone depths are not constant but depend on the external environment, drying–wetting time ratio and concrete

* Corresponding author. School of Civil Engineering, Central South University, 22 Shaoshan Road, Changsha 410075, China.
E-mail address: 23671871@qq.com (Z. Yu).

http://dx.doi.org/10.1016/j.cemconcomp.2016.06.011
0958-9465/

properties [15]. Hence, it is appropriate to determine the chloride convection zone depth on the basis of traditional approaches, i.e. fitted by the measured data, rather than recommended constant values. However, the traditional approaches to determine the depth of chloride convection zone also have an insuperable weakness, that field measured data should be first obtained prior to deducing the chloride profiles. Therefore, traditional approaches are unsuitable for newly constructed concrete structures which have not formed a stable chloride convection zone and lack long-term measured data. To date, there are few references on the solution methods and models for estimating chloride convection zone depth in concrete. Consequently, accurate determination of the chloride convection zone depth in concrete is important for the durability of RC structures.

This study proposes a model of chloride convection zone depth in RC based on a hypothesis of linear variation of chloride concentration and water influential depth in convective zones. The results aim to provide a theoretical and technical clue to investigate the durability of RC in marine environments.

2. Model of chloride convection zone depth in concrete

Under dry–wet cycling environments, chloride migration in concrete can be divided into two typical zones, namely, convection zone and diffusion area. The formation and development of these two zones are usually dominated by environmental conditions and concrete characteristics. The convection action has an obvious effect on chloride transports in the surface region of concrete covers, which forms the convection zone. In contrast, the diffusion process plays a dominant role in the depths of concrete, which is defined as diffusion zone. On the basis of several assumptions (e.g., constant chloride diffusion coefficient in time and space domain, constant chloride concentration at the surface and occurrence of chloride diffusion in a semi-infinite medium), Fick's second law of diffusion is commonly employed to represent the chloride concentration profile in concrete [16,17] (Eq. (1)). Based on the boundary condition (i.e., $C(0,t) = C_s$) and initial condition (i.e., $C(x,0) = C_0$), the corresponding analytical solution of Eq. (1) can be obtained and expressed in Eq. (2) by using the error function.

$$\frac{\partial C}{\partial t} = \frac{\partial}{\partial x}\left(D\frac{\partial C}{\partial x}\right), \tag{1}$$

$$C(x,t) = C_0 + (C_s - C_0)\left[1 - erf\left(\frac{x-\Delta x}{2\sqrt{Dt}}\right)\right], \tag{2}$$

where $C(x,t)$ represents the chloride concentration at the depth x and at the exposure time t. C_s and C_0 are the chloride concentration and initial chloride concentration at the surface of concrete, respectively. D represents the chloride diffusion coefficient, and Δx corresponds to the convection zone depth of chloride. *erf* denotes the statistical error function.

As shown in Eq. (2), the error function term has three main governing parameters, i.e. the surface chloride concentration C_s, chloride convection zone depth Δx and chloride diffusion coefficient D. An accurate prediction of the chloride convection zone depth is still an issue for investigating the durability of concrete in marine environments, although there are many effective solutions for chloride diffusion coefficient [18]. The depth of the maximum chloride concentration in concrete is defined as the chloride convection zone depth which can be determined by the fitting profiles of Eq. (3) based on measured data. However, this method does not suit to newly built constructions and existing structures without steady surface chloride concentration. The chloride diffusion coefficient, initial chloride concentration and surface chloride concentration in concrete are always assumed to be constant. By measuring the chloride concentration at depth x for different times t_1 and t_2, the chloride convection zone depth can be deduced from Eq. (2) as:

$$\frac{C(x,t_1) - C(x,t_2)}{C_s - C_0} = erf\left(\frac{x-\Delta x}{2\sqrt{Dt_2}}\right) - erf\left(\frac{x-\Delta x}{2\sqrt{Dt_1}}\right). \tag{3}$$

As a traditional approach for determining the chloride convection zone depth, it has some defects, e.g. time-consuming and dependence of field measurement. Li et al. [13] regarded the water influential depth as the convection zone depth. This approach, however, does not apply to practical cases. Under continuous cycles of wetting–drying, chloride-ion-containing water is absorbed by the capillary suction of unsaturated concrete. If the quantity of water in concrete cannot sustain pore water to connect, the inner liquid water may transfer into external air in terms of water vapour. Thus, the remaining salt solution in concrete pore evaporates and concentrates, and the chloride concentration increases on the surface of concrete. Owing to the effects of hysteresis and blocking, the water evaporation only affects a certain range of depths in concrete. Hence, the corresponding chloride convection zone depth on concrete surface is less than the recommended value in the reference [15]. Considerable chloride also ingresses into the concrete under continuous cycles of wetting–drying, and thus the chloride concentration at a certain depth reaches a quasi-equilibrium state. Thereupon, the maximum chloride concentration and the corresponding convection zone depth appear. There are few approaches on the identification of chloride convection zone depth. In this study, the chloride convection zone depth in concrete is determined on the basis of a linear variation hypothesis of chloride concentration and water influential depth in convective zones. Fig. 1 illustrates the model of chloride convection zone depth on the surface of concrete. The variation of water influential depth

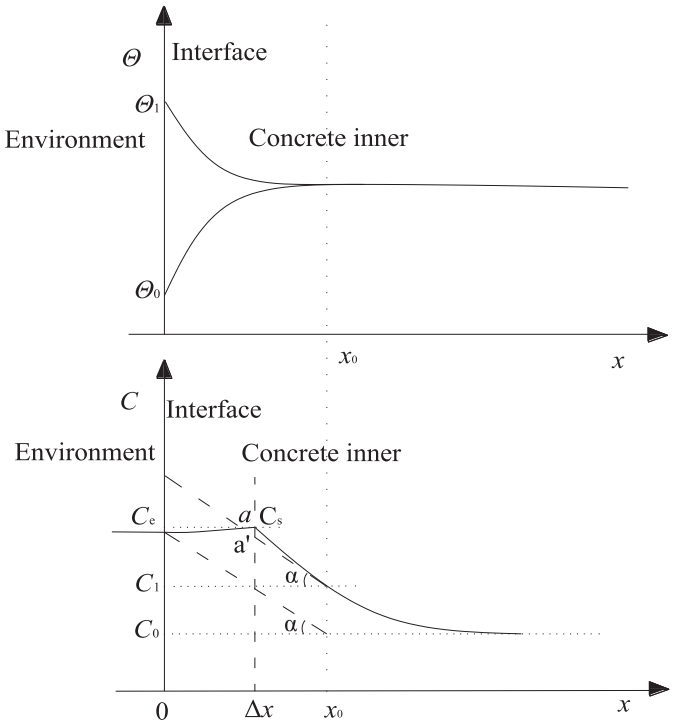

Fig. 1. Convection zone depth model of chloride in concrete surface.

and chloride content are plotted in the top and bottom portion of Fig. 1, respectively.

According to Fig. 1, the correlation between water influential depth and chloride convection zone depth can be expressed in Eq. (4). This correlation is based on the linear variation hypothesis of chloride concentration and water influential depth within the convection zone of concrete. In this study, the equivalent chloride concentration of external environment on the concrete surface is defined as C_e. The corresponding chloride concentrations at a water influential depth x_0 and chloride convection zone depth Δx are denoted as C_1 and C_s, respectively. The parameter α is defined as the angle of the chloride concentration curve at water influential depth with the horizontal line.

$$\mathrm{tg}\alpha = \frac{C_e - C_0}{x_0} = \frac{C_s - C_1}{x_0 - \Delta x}. \tag{4}$$

By rewriting Eq. (4), the chloride convection zone depth Δx yields:

$$\Delta x = \left(1 - \frac{C_s - C_1}{C_e - C_0}\right) x_0. \tag{5}$$

In this model, given that the initial chloride concentration C_0 can be directly obtained by measured data, the remaining variables such as C_e, C_1 and C_s need to be determined. If the water influential depth x_0 is numerically simulated, the chloride convection zone depth Δx at different conditions can be calculated by Eq. (5). When the time is beyond a certain value, parameters C_e, C_1 and C_s can be considered constant. As shown in Eq. (5), the chloride convection zone depth Δx is expressed as a function of water influential depth x_0, which is different from the traditional concept by regarding it as constant. In the subsequent sections, the determination of the parameters x_0, C_e, C_1 and C_s, will be discussed.

2.1. Water influential depth x_0

In this work, the water influential depth x_0 is determined using finite difference method [13,15]. The wetting process of tests is defined as the direct spraying of liquid water from simulation environment chamber to the concrete surface, while the corresponding drying process is regarded as the case that the relative humidity of simulation environment chamber is less than that of concrete surface. The transmission mechanism of water on concrete surface during wetting process is capillarity, and diffusion for the drying process. Owing to the difference in the water transmission mechanism between the drying and wetting processes, the corresponding transmission coefficients differ from each other. Under continuous cycles of wetting and drying, the water transmission flow J_w can be represented by Eq. (6) and the corresponding diffusion coefficients $D(\theta)$ can be expressed as Eq. (7). The water transmission process between concrete and the external environment is generally unsteady. In most cases, it is difficult to directly measure the water diffusion coefficient of the wetting process. Nevertheless, the relation between water adsorption and diffusion coefficient can be indirectly determined by Eq. (8) [19], and the water diffusion coefficient for the drying process proposed by the CEB-FIP Model Code can be obtained by the S-curve [20]. The water saturation in concrete during the numerical simulation of water transport is described by Eq. (9), and the corresponding initial condition can be expressed by Eq. (10).

$$J_w = -\rho_l \phi D(\theta) \nabla\theta, \tag{6}$$

$$D(\theta) = \begin{cases} D_d(\theta) = D_d^s \left(\alpha_0 + \dfrac{1-\alpha_0}{1 + \left(\dfrac{1-\theta}{1-\theta_c}\right)^N}\right); & \text{Drying process,} \\ D_w(\theta) = D_w^0 \exp(n\theta); & \text{Wetting process} \end{cases} \tag{7}$$

$$\left(\frac{S_0}{\phi}\right)^2 = D_w^0 \left(\exp(n)\left(\frac{2}{n} - \frac{1}{n^2}\right) - \left(\frac{1}{n} - \frac{1}{n^2}\right)\right), \tag{8}$$

$$\phi = \frac{\rho_c (m_w - m_d)}{\rho_w m_d} \times 100\%, \tag{9}$$

$$\theta(x, t = 0) = \theta_{ini}(x), \tag{10}$$

where D_w^0 and D_d^s are the water diffusion coefficients of concrete under completely drying and wetting conditions, respectively; $D_w(\theta)$ represents the water diffusion coefficient of concrete under water saturation, θ; t is the water transport time; θ is the pore water saturation (in a range of 0–1) of concrete; $\nabla\theta$ is the gradient of water saturation; S_0 is the water adsorption coefficient; ρ_l is the density of liquid water; ϕ is the porosity of concrete; m_w and m_d are the weight of concrete under complete wetting and drying conditions, respectively; ρ_w and ρ_c are the corresponding densities of concrete, respectively; n stands for the regression coefficient with a recommended value ranging from six to eight; α_0, θ_c and N are the regression coefficients as recommended in the CEB-FIP Model Code.

Computer programs are compiled to determine the water saturation distribution in concrete. Thus, the water influential depth x_0 can be determined by comparing the changes of water saturation distribution during the drying and wetting processes. The details can be found in Ref. [15].

2.2. Surface chloride concentration C_s

The maximum surface chloride concentration on the concrete surface is typically considered as the demarcation point between the convection zone and diffusion area [8], which is a function of internal and external factors, e.g. solution concentration, environmental loads and concrete composition [21,22]. The change of surface chloride concentration is an accumulation process under the coupled effects of multiple factors [23]. According to existing studies, the surface chloride concentration in concrete follows a log-normal or normal function, extreme value form [24–26], etc. However, these studies are incompatible mathematical models. In this study, the influence of marine environment on the chloride concentration in concrete structures is assumed to be related to the elevation and linear distance from the seaside. When the linear distance from the seaside is beyond a certain value, the chloride concentration in an atmospheric environment is irrelevant to the elevation. If the surface chloride concentration in concrete is set as a function of the linear distance from the seaside l, their relation can be described as:

$$C_s = C_s(l). \tag{11}$$

According to the surroundings in the vertical direction, a concrete structure near the seaside can be divided into atmospheric, underwater, splash and tidal zones. Therefore, the surface chloride concentration in concrete implies special characteristics for different zones. Diffusion is usually the transport mechanism of chloride ingressing into concrete underwater. Therefore, the

surface chloride concentration C_s is equal to the seawater chloride concentration. At the other three zones, chlorides mainly ingresse into concrete by capillary action. The values of surface chloride concentration C_s are thus determined based on the water saturation of concrete, drying–wetting time ratio, equivalent chloride concentration of external environment C_e, etc.

The water saturation of concrete is expressed as a function of drying–wetting time ratio. Given that the drying–wetting time ratio depends on tidal cycles, the influences of the water saturation and drying–wetting time ratio on surface chloride concentration C_s can be deduced as a function of elevation h. A concrete structure also adsorbs chloride from the external environment. Hence, the equivalent chloride concentration of the external environment C_e is associated with elevation h. As discussed above, the surface chloride concentration of concrete depends on elevation h, i.e.,

$$C_s = C_s(h). \tag{12}$$

Considering the hypothesis of constant surface chloride concentration in concrete, previous studies have deduced the corresponding results. In most realistic cases, the surface chloride concentration of concrete exposed to marine environment initially changes with time and chloride concentration [27] and then becomes constant. There are many time-dependent models for the surface chloride concentration of concrete, e.g., linear, polynomial, square root, power function, logarithm and exponential types [28–32]. However, the applicability of these models is vague due to their restricted theory (Fick's second law of diffusion) or basis on statistics experience law alone. The corresponding assumptions are logically inconsistent. Pack et al. [33] indicated that C_s was a logarithm function of time, and a build-up of C_s was to calculate a chloride profile by using the best fit of a change in C_s with time from field data as Eq. (13). LIFE 365 also indicated a constant C_s.

$$C_s = \alpha[\ln(\beta t + 1)] + k, \tag{13}$$

where t is the exposed time in years; α, β and k are constants obtained from the in-situ environment.

Based on a review of existing theories and preceding discussions [34], this study describes the surface chloride concentration in concrete by the exponential function model:

$$C_s(t) = C_0 + C_{\max}(1 - e^{-rt}), \tag{14}$$

where $C_s(t)$ represents the surface chloride concentration of the concrete surface at time t; C_0 and $C_{\max}$ represent the initial chloride concentration and the surface chloride concentration in concrete at a steady state, respectively; r is the fitting coefficient.

As mentioned above, the surface chloride concentration in concrete can be defined as a function of distance, elevation and time:

$$C_s(t, h, l) = f(C_s(l), C_s(h), C_s(t)). \tag{15}$$

2.3. Equivalent chloride concentration of the external environment on concrete surface C_e

The chloride concentration of an external environment C_{envi} is defined as the chloride concentration of salt solution or seawater when concrete is immersed in a salt solution or underwater zone. The corresponding equivalent chloride concentration of an external environment on a concrete surface C_e can be expressed by Eq. (16). For concrete in the atmospheric/splash/tidal zones near the seaside, owing to the external environment imposing the same C_{envi} on concrete for the same location, C_e can be directly determined by utilising existing RC structures for a long time. These RC structures are defined as third-party reference. Firstly, the chloride concentration distribution in concrete can be measured to plot the chloride concentration profile. Secondly, the water influential depth $x_{0,a}$ can be obtained through the method in Subsection 2.1. Thirdly, the parameters of the third-party reference, such as surface chloride concentration $C_{s,a}$, initial chloride concentration $C_{0,a}$, chloride convection zone depth $\Delta x_{0,a}$ and chloride concentration $C_{1,an}$ at water influential depth $x_{0,a}$, can be deduced by using Eq. (2). Finally, by substituting the parameters of the third-party reference into Eq. (5), the equivalent chloride concentration of external environment C_e can be rewritten as:

$$C_e = C_{envi}{}^{v}/_{\rho_r} = \begin{cases} C_{sol}{}^{v}/_{\rho_r}; & \text{(underwater zone)} \\ \left[C_{0,a} + (C_{s,a} - C_{1,a})\dfrac{x_{0,a}}{x_{0,a} - \Delta x_{0,a}}\right] \cdot \dfrac{v\rho_{r,a}}{v_a \rho_r}; & \text{(atmospheric/splash/tidal zone)} \end{cases}, \tag{16}$$

where C_{sol} is the chloride concentration of salt solution or seawater in the environment; v and v_a denote the porosities of concrete and the third-party reference, respectively; ρ_r and $\rho_{r,a}$ represent the specific gravities of concrete and the third-party reference, respectively.

2.4. Chloride concentration at water influential depth C_1

For long-term field engineering, if the chloride concentration at water influential depth C_1 can be measured from concrete, the convection zone depth Δx may be directly determined by substituting C_1 into Eq. (5). However, for new RC structures, it is difficult to determine C_1 because of its instability. Therefore, a novel method is proposed in this study to predict C_1. It is based on the time-dependent chloride diffusion coefficient D_t (Eq. (17)) proposed by Michael et al. [23] which is considered as constant D_{t0} when the exposed time t is beyond a certain time t_0 (e.g. 20 or 30 years). Given that the surface chloride concentration C_s tends to be constant, a quasi-equilibrium state can be reached between the ingressing of chlorides into the concrete surface from the external environment and the diffusing of chlorides to the inner concrete from the concrete surface. Hence, if we assume that the chloride concentration C_1 at water influential depth x_0 tends to be constant at the same time t_0 (i.e., 20 or 30 years), C_1 can be determined by Eq. (18).

$$D_t = D_{28}\left(\frac{t_{28}}{t}\right)^m, \tag{17}$$

$$C_1 = C(x_0, t_0) = C_0 + (C_s - C_0)\left[1 - erf\left(\frac{x_0 - \Delta x}{2\sqrt{D_{t0} t_0}}\right)\right], \quad (18)$$

where D_t is the diffusion coefficient at time t; D_{28} is the diffusion coefficient at time $t_{28} = 28$ days, and m is constant.

By substituting Eq. (18) into Eq. (5), the chloride convection zone depth Δx can be determined by approximate analysis methods.

3. Experimental procedures

3.1. Raw materials and mix proportions of concrete

Raw materials including ordinary Portland cement (P·O 42.5 grade), water reducing agent of polycarboxylic series, river sand and water were utilised throughout this work. Limestones were used as coarse aggregate with sizes ranging from 5 mm to 20 mm. Table 1 presents the mix proportion of concrete.

3.2. Preparation of test specimens and techniques

Concrete was mechanically mixed until complete homogeneity was achieved. Specimens of sizes of 150 mm × 150 mm × 150 mm and 150 mm × 150 mm × 400 mm were prepared. After casting, all moulded specimens were surfaced with plastic sheets and cured indoors with temperature of 20 °C and relative humidity of 98% for 24 h. The specimens were then removed from the moulds and immersed in saturated limewater (at 20 ± 2 °C) for 27 days.

All sides of the concrete specimens were sealed by epoxy, leaving one side unsealed for testing. An artificial simulation environment test was conducted with three stages for a cycle, and the corresponding temperature and duration were set as 40 °C for 30 h, 50 °C for 30 h and 60 °C for 12 h. The wetting process was conducted at 40 °C for 50 min by spraying salt solution. The remaining time was used for the drying process with a relative humidity of 70%. The concentration of the salt (i.e., sodium chloride) solution was 5%, and the wind speed was set as 3 m/s. Fig. 2 shows the environmental simulation of test systems.

An automatic grinding machine with a type of PF-1100 (produced by Germann Co. in Denmark) was used to manufacture the concrete powder. Fig. 3 shows the characteristic of the measured specimens. The concrete powder was grinded in an agate mortar again, and its fineness was ensured to pass through 75 μm sieve. The chloride concentration of concrete was tested in accordance with the standard test JTJ 270–1998 of China. The steps are presented as follows. Firstly, the fabricated samples of concrete powder were soaked in water at room temperature for 24 h. Secondly, the solution was vacuum filtration, and the solid powder filtered out was repeated washing. Finally, a certain solution was taken out and titrated by silver nitrate solution, and the chloride concentration is calculated as:

$$P = \frac{C_{AgNO_3} V_5 \times 0.03545}{G \times \frac{V_4}{V_3}} \times 100\%, \quad (19)$$

where P is the chloride concentration in %; C_{AgNO_3} is the concentration of silver nitrate solution in mol/L; G is the weight of sample in gram; V_3, V_4 and V_5 are the volumes of water for soaking the sample, the water for titration every time, and the silver nitrate solution for titration every time, in mL, respectively.

The water characteristic curve of concrete was investigated by utilising different types of saturated salt solutions to provide a diverse relative humidity environment in this study [13,15]. Chips of concrete in thicknesses of 3 mm–5 mm, length of 100 mm and width of 100 mm were prepared to investigate the moisture adsorption and desorption curves. To reach the equilibrium state, the specimens specified for this study were placed in different types of relative humidity environment for 3 months. The weights of chips were measured periodically. Wetting tests of concrete samples were conducted as follows. Firstly, concrete samples with one unsealed side dried to constant weight were placed into a plastic container. Secondly, water was poured into the container with a level of 2 mm. Finally, the concrete samples were taken out, wiped dry and accurately weighed. After the wetting test, drying tests were conducted in a thermostatic chamber with a fan to dry the concrete samples, and the weights of samples were measured at different times. The concrete samples were dried for seven days using a vacuum drying oven at room temperature to determine their dry weight m_r. The fully saturated wet weight m_s was measured by soaking the samples into water for 72 h. If the wet concrete weight m under different relative humidity can be directly weighed, the corresponding water saturation Θ of the concrete samples is calculated as:

$$\Theta = \frac{m - m_r}{m_s - m_r}. \quad (20)$$

4. Results and discussion

4.1. Surface chloride concentration in concrete with elevation and linear distance from the seaside

This study investigates the dependence of chloride concentration of concrete on elevation h. Field tests were therefore carried out, and the trestle was chose as a research object. Fig. 4 shows the variation of the chloride concentration in concrete against elevation. Fig. 5 presents the profiles of surface chloride concentration and the diffusion coefficient in concrete varying with elevation. The maximum chloride concentration curve on the concrete surface with linear distance from the seaside is plotted in Fig. 6. In this section, the elevation data were transformed on the basis of a nearby tidal station, i.e., the elevation of the gauging points were calculated as the height from the sea level plus the relative value of 1 m. The experimental data were fitted based on Fick's diffusion law, and the calculation parameters are obtained on the basis of the above criterion and the measured data.

Fig. 4 indicates that the chloride concentration in concrete of the trestle varies with increasing elevation h. When concrete was close to the sea level (e.g. 1.1 m), the chloride concentration sustained a constant value within a certain depth (approximately 2.5 mm), and the maximum chloride concentration existed at the corresponding depth. The change law of chloride concentration within the corresponding depth can be described by Fick's diffusion law. If concrete

Table 1
Mix proportion of concrete/(kg.m^{-3}).

Concrete grade	Cement	Slag	Fly ash	Sand	Coarse aggregate	Water	Water reducing agent
C20	220	65	60	780	1030	176	3.9
C50	375	85	35	720	1085	152	5.0

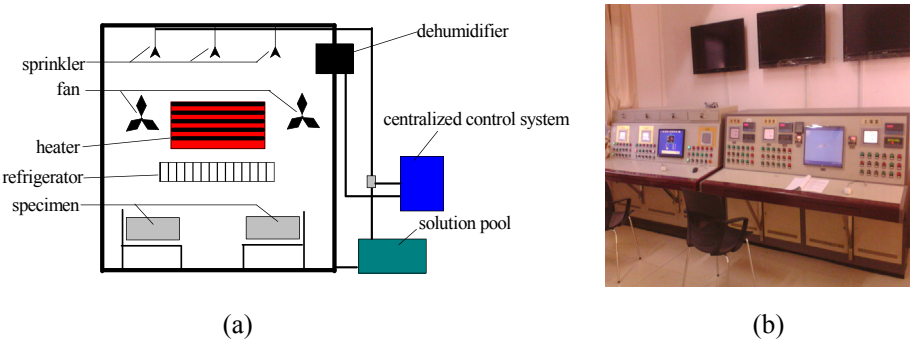

Fig. 2. Environmental simulation test system. (a) Environmental test chamber; (b) Centralized control system.

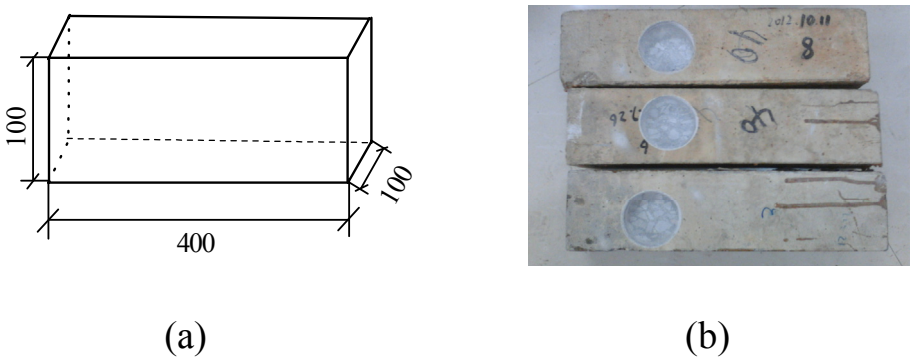

Fig. 3. Characteristic of the measured specimen. (a) Size of the specimen; (b) Profile of the measured specimen.

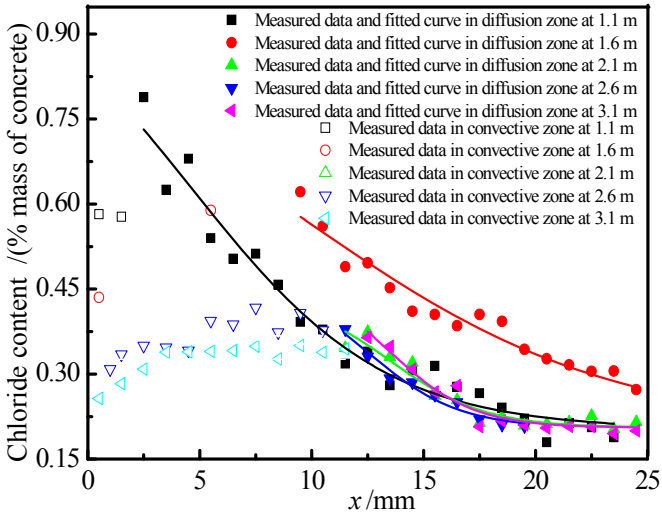

Fig. 4. Curves of the chloride concentration in concrete with elevation.

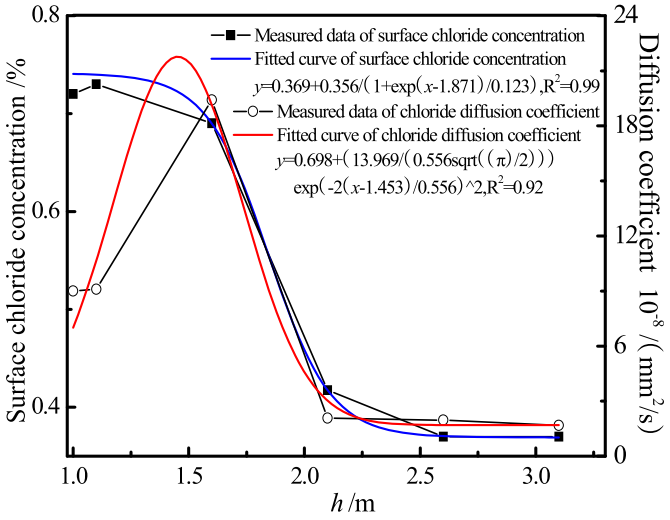

Fig. 5. Curves of the surface chloride concentration and the chloride diffusion coefficient with elevation.

located in the tidal zone and splash area (e.g. 1.6 m), the variation trend of the chloride concentration in concrete was similar to the above-mentioned situation, but the chloride convection zone depth and the chloride concentration in concrete increased significantly. Although the liquid water in concrete pores transmitted into atmosphere in forms of vapour during the drying process, chlorides were retained in concrete. Under the effects of concentration and re-crystallisation, chloride concentration increased within a certain depth of concrete surface. In this case, chloride probably diffused from interior to exterior. At the initial period of the wetting process, the chloride concentration in concrete pores was higher than spraying salt solution which was caused by water evaporation during the drying process. Consequently, chloride diffused on the concrete surface as well. During the drying–wetting cycles, increasing chloride ingressed into concrete, and a quasi-equilibrium state of the chloride concentration in a certain depth of concrete surface then appeared. Therefore, there were critical values of the chloride concentration and the convection zone depth. This case only applies to concrete surface and never occurs inside the concrete because of the hysteresis effect of diffusion and

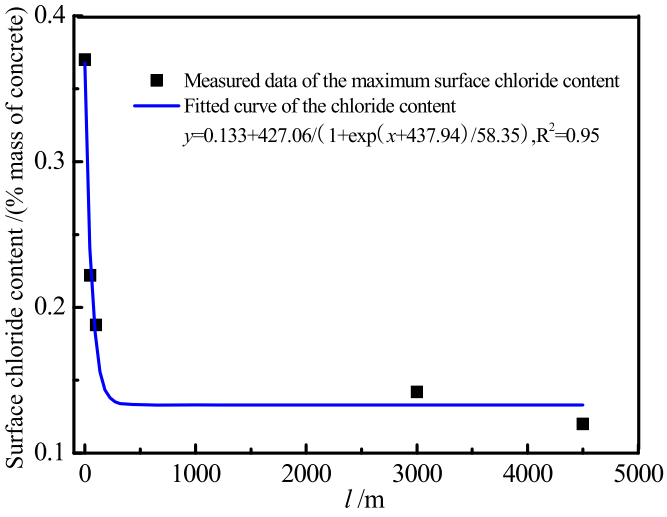

Fig. 6. Curve of surface chloride concentration in concrete with distance from seaside.

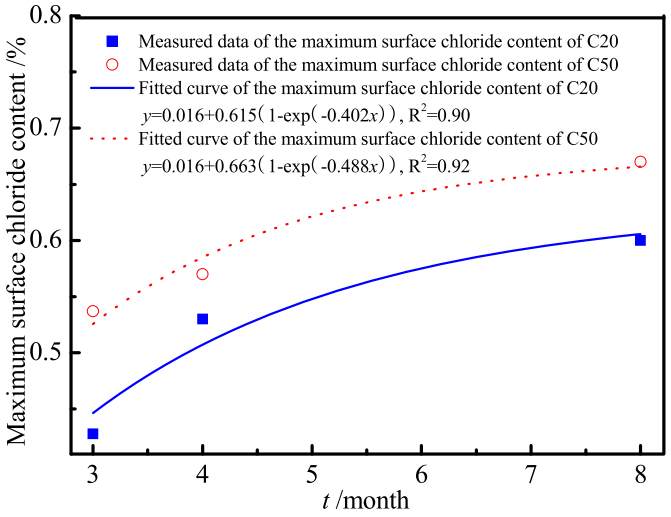

Fig. 7. Surface chloride concentration in concrete with time.

the blocking effect of concrete. Fick's diffusion law thus suits to depict the changes in the chloride concentration inside the core zone of concrete. Surface chloride concentration in the atmospheric zone (e.g. 2.1, 2.6 and 3.1 m) was basically constant. The variation of the chloride concentration of field measurement fitted well with Fick's diffusion law only when the depth was more than a fixed value. This phenomenon may be due to the fact that the chloride sources of concrete surface in atmospheric zone are sea fog, rain and air from the sea which contain minimal chloride and generate low concentration gradients and diffusion forces. On the basis of the chloride concentration of concrete surface at 2.1 m and Eq. (16), the calculated equivalent chloride concentration of external environment on concrete surface C_e is approximately 0.4%.

To discuss the influence of elevation on chloride concentrations, the following sections investigate the changes of surface chloride concentration and the chloride diffusion coefficient in concrete against elevation, as shown in Fig. 5.

According to Fig. 5, the surface chloride concentration and the chloride diffusion coefficient in concrete changed with increasing elevation, and the mechanisms differed from each other. The surface chloride concentration in concrete increased with elevation, but reduced when the elevation is beyond a certain value. The entire changing rule can be described by S-curve which is given in Eq. (21). The chloride diffusion coefficient in concrete will increase first and decrease afterward, and the change law can be depicted by a Gauss function, which is stated in Eq. (22).

$$y = a + b/(1 + \exp((x - x_0)/c)), \tag{21}$$

$$y = y_0 + \frac{a}{b\sqrt{0.5\pi}}\exp\left(-2\left(\frac{x - x_0}{b}\right)^2\right). \tag{22}$$

The change of the surface chloride concentration in concrete with distance from seaside l was also investigated, and the corresponding profile was plotted in Fig. 6.

Fig. 6 illustrates that the surface chloride concentration in concrete apparently decreases with increasing distance from seaside, and it tends to be constant when the distance is beyond a fixed value. The main reason for the above phenomenon is that the surface chloride content in concrete is a constantly absorbed and accumulated process of chloride from atmosphere, sea fog and rainfall. For an increasing distance from the sea, the chloride concentration in atmosphere decreases and tends to be constant. A threshold thus exists. Moreover, Fig. 6 shows that their correlation can be described by Eq. (21).

4.2. Time-dependence of surface chloride concentration in concrete

This study used different types of concrete with grades of C20 and C50 to investigate the consistency of the time-dependence of the surface chloride concentration in concrete under natural or artificial simulation environment. The corresponding variations with time are shown in Fig. 7.

Fig. 7 shows that the surface chloride concentration in concrete increases and tends to be constant when it is beyond a certain value (i.e. threshold). The measured data agreed well with the fitted curve, which implied that the modified exponential function given as Eq. (14) suited to illustrate the variation of chloride concentration against time. The surface chloride concentration in concrete was an accumulated process in artificial simulation environment, and tended to be in an equilibrium or quasi-equilibrium state. The surface chloride concentration in concrete of different strength grades differed due to the variances of the micro structure and the porosity of concrete. Micro pore percentages increased with increasing concrete strengths, and the corresponding capillary action became obvious. Hence, considerable chlorides can be absorbed into concrete. Although low-strength-grade concrete was highly porous which can concentrate and enrich considerable chlorides, the dominant factor of chloride ingress is the capillary action, i.e. the less the micro pores in low-strength-grade concrete, the fewer the chlorides absorbed on concrete surface.

4.3. Convection zone depth of chloride in concrete

Prior to determining the convection zone depth of chloride on concrete surface, the water influential depth x_0 should be obtained. On the basis of finite difference methods, the simulation procedure is compiled in this work [15]. The numerical simulation method and data from the field measurements were used to calibrate the performance of the proposed model. Considering that the numerical simulation used the water saturation of concrete to describe the change in water content which can be tested by humidity sensor in forms of relative humidity, the corresponding correlation between the relative humidity and the water saturation should be determined firstly. In this study, numerical simulations were conducted using concrete with a grade of C50. Fig. 8 presents the

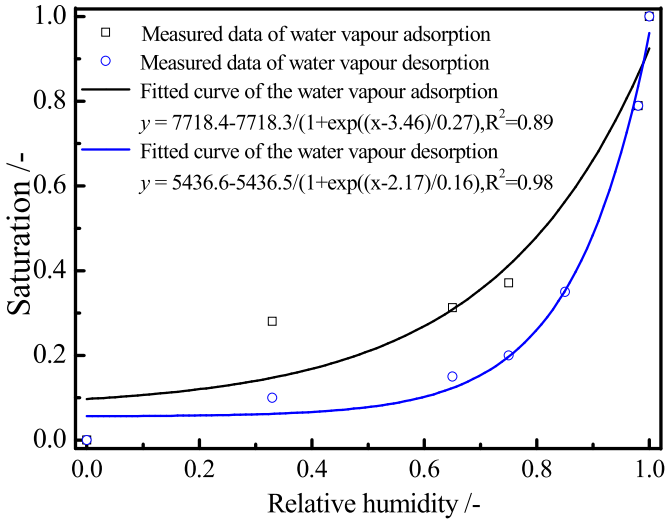

Fig. 8. Correlation curves of the relative humidity and the water saturation in concrete.

corresponding correlation between the relative humidity and the water saturation in concrete.

As shown in Fig. 8, the water saturation of concrete increased with increasing relative humidity, and a good correlation curve in terms of Sigmoidal model was established. The adsorption–desorption curves were obviously divided into two segments and a closed loop formed. The adsorption curve did not coincide with the desorption curve, which may be caused by ink–bottle pores [35]. The correlation between water saturation and relative humidity provides a basis for the following numerical simulation. The water saturation was set as a variable to describe the water influential depth on concrete surfaces. The water loss and adsorption coefficient should also be determined. Fig. 9 shows the variation of the water adsorption and the water loss of concrete surface against time.

Fig. 9 shows that the amount of water adsorption and water loss with square root of time manifest as a linear function, and the measured data agree well with the fitting curve. The water adsorption coefficient of concrete surface fitted by the fitting curve slope was approximately 9.1 $\times$ 10^{-6} m/$s^{0.5}$. The water diffusion coefficient obtained by Eqs. (8) and (9) was approximately 4.9 $\times$ 10^{-11} m^2/s. The water loss ratio fitted by the drying process was approximately 1 g/$h^{1/2}$. The corresponding water diffusion coefficient of concrete under complete wetting condition determined using Eqs. (6) and (7) was approximately 2 $\times$ 10^{-10} m^2/s.

To validate the rationality of the numerical results, drying–wetting tests were conducted on concrete specimens in an artificial environmental system. The relative humidity in concrete specimens was measured periodically. The parameters for the drying test process were presented as follows: the relative humidity of the artificial environment of approximately 70%, the wind speed of 3 m/s, and the temperature of 25 °C. The amount of spray water was approximately 30 mL/(cm^2·min) during the wetting process, and the drying–wetting test was conducted for 2 weeks. The hypothesis conditions of the numerical simulation were presented as follows: the relative humidity of the environment was 70% during the drying process, the initial water saturation of concrete was taken as 1.0, the relative humidity of the environment was regarded as the equal value of concrete surface, the concrete surface was assumed to be water saturation at the initial moment,

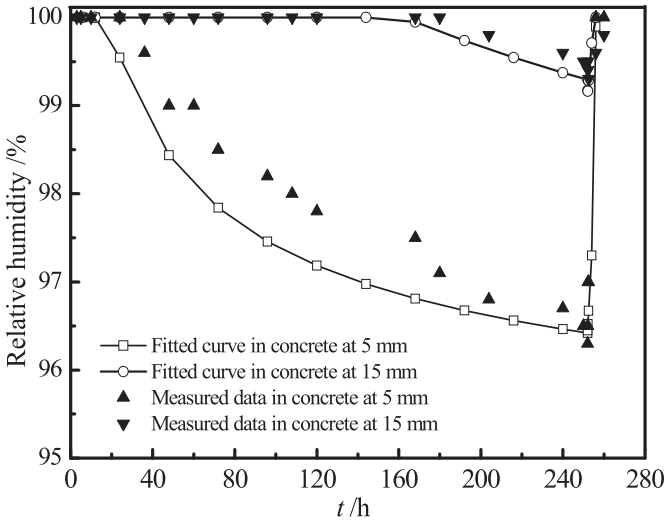

Fig. 10. Curves of the relative humidity in concrete under drying-wetting condition.

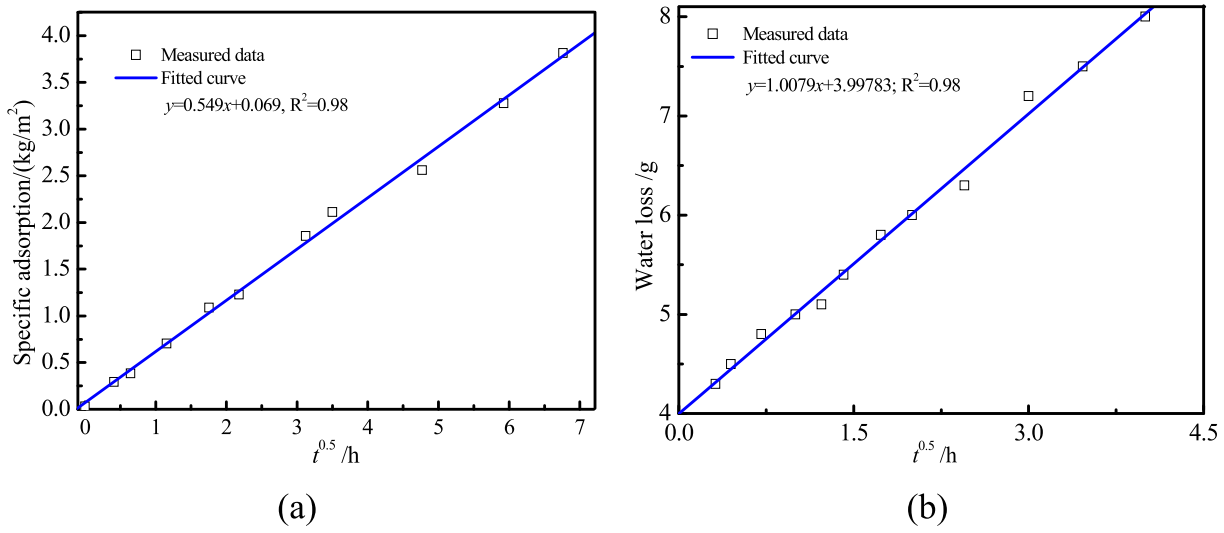

Fig. 9. Curve of the water adsorption and water loss of concrete surface with time. (a) Specific water adsorption; (b) Water loss.

and the water diffusion coefficients were from the obtained values in Fig. 9. The variation of the relative humidity in concrete under drying–wetting conditions is plotted in Fig. 10.

According to Fig. 10, the relative humidity in concrete changed slowly with time during the drying–wetting process. The values of relative humidity were different at different depths of concrete, although the mechanisms were similar. The changing of relative humidity with time during the wetting process was faster than that during the drying process which could be caused by different transport mechanisms. Fig. 10 also implies that although the tendency of the measured data and the fitted curve are similar, the values may be different. This difference could be caused by the error of sensors and the number of the test cycles which affects the equilibrium state of the humidity. However, the proposed numerical method is suitable to determine the water distribution in concrete.

In view of the preceding discussion, the rationality of the chloride convection zone depth on the surface of concrete under artificial simulation environments will be verified later. The simulation parameters of the drying process were presented as follows: the initial water saturation of concrete of 0.8, and the corresponding water saturation of the environment transformed from relative humidity of 0.4. Fig. 11 shows the variation of the water saturation distribution in concrete under a simulation environment. The initial chloride concentration of concrete was approximately of 0.016%, and the measured density of concrete was approximately 2.4 g/cm^3.

As shown in Fig. 11, the water saturation distribution in concrete only changed in a certain depth range of x_0 during the drying–wetting process, and the water saturation distribution in concrete was basically not changed when the depth was beyond x_0. On the basis of these assumptions, the water influential depth x_0 in concrete under the artificial simulation environment can be calculated by the theoretical model as approximately 14 mm. The use of the water influential depth x_0 in determining the chloride convection zone depth Δx will be discussed later. Fig. 12 shows the chloride concentration of concrete under artificial simulation environment for 8 months.

In Fig. 12, a critical depth divided the chloride distribution on concrete surface into diffusion zones and convection areas. In the diffusion zone, the chloride transport mechanism was diffusion and the fitted curve based on Fick's second law agreed well with field experimental data. Fick's diffusion law, i.e. Eq. (2), indicated that

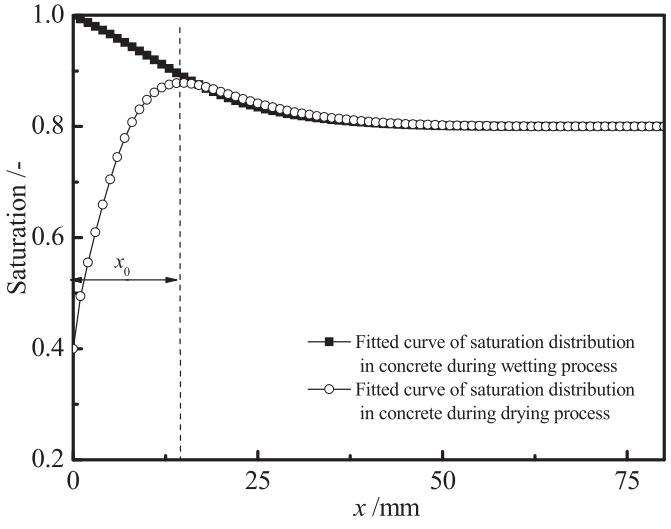

Fig. 11. Curve of water saturation distribution in concrete under artificial simulation environment.

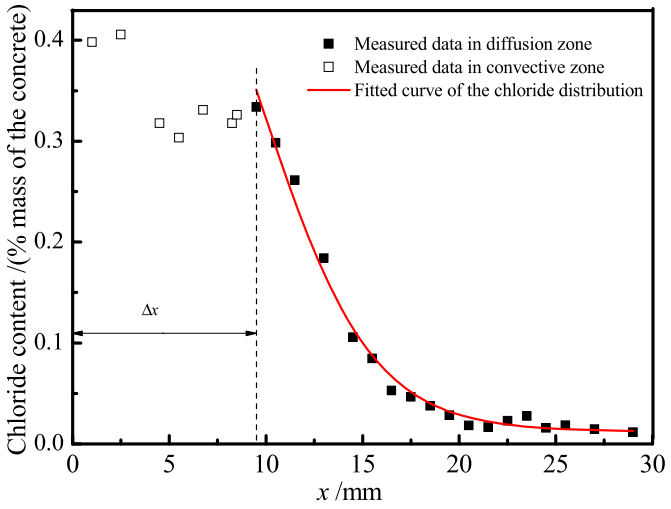

Fig. 12. Chloride concentration curve of concrete under artificial simulation environment.

the chloride convection zone depth Δx on concrete surface was approximately 10 mm. Although this approach was utilised to obtain the chloride convection zone depth Δx under the corresponding environment, it still had many deficiencies that limited its applications, e.g. time-consuming, requiring measured results and not suitable for new RC structures.

A novel chloride convection zone depth model was proposed in this work to overcome the shortcomings of the traditional solution. According to Eq. (5), the theoretical calculation result of the chloride convection zone depth Δx on the concrete surface was approximately 11 mm, which was close to the calculated value by Fick's second law of diffusion. Their difference could be caused by different hypothesis bases. The convection zone depth model of chloride on concrete surface was based on the assumption of linear variation of the chloride (as shown in Fig. 1) which decreased the real chloride concentration in concrete during calculation. Consequently, the final result exaggerated the chloride convection zone depth. According to Eqs. (5) and (16), the corresponding equivalent chloride concentration of external environment on concrete surface C_e was approximately 0.95%. It is evident by comparing both results that the proposed model in this study for determining chloride convection zone depth is reasonable.

By using a trestle served in Zhuhai Port for 12 years as an example, the applicability of the chloride convection zone depth model was verified in this paper. The sea current was irregular semidiurnal tide, and the measured seawater salinity of 2.9% was regarded as the chloride salt concentration. The testing points located in splash zones, and the corresponding wetting time ratio defined as the ratio between the wetting and drying times for the entire year was approximately 0.776 (as shown in Table 2). The numerical result of water influential depth x_0 was approximately 6 mm, and the variation of the chloride concentration distribution in concrete of trestle is shown in Fig. 13.

From Fig. 13, the chloride concentration in concrete can be represented by Fick's diffusion law when the depth is beyond a certain value, and the measured data accord well with the fitting curve. The chloride concentration remains constant in a certain depth range of concrete surface. Thus, the concrete surface can be divided into diffusion area and convection zone on the basis of chloride concentration. The corresponding critical depth is regarded as the chloride convection zone depth. Fig. 13 also illustrates that the chloride convection zone depth Δx on the concrete surface

Table 2
Wetting time ratio for different position of concrete in situ environment.

Elevation	Month												Average value
	1	2	3	4	5	6	7	8	9	10	11	12	
1.1 m	0.728	0.783	0.796	0.705	0.761	0.826	0.751	0.777	0.716	0.837	0.836	0.791	0.776
1.6 m	0.315	0.316	0.316	0.369	0.337	0.307	0.36	0.348	0.419	0.413	0.414	0.434	0.362
2.1 m	0.103	0.083	0.096	0.099	0.118	0.107	0.108	0.165	0.14	0.13	0.129	0.106	0.115
2.6 m	0.016	0	0	0	0	0	0	0	0	0	0	0	0.001
3.1 m	0	0	0	0	0	0	0	0	0	0	0	0	0

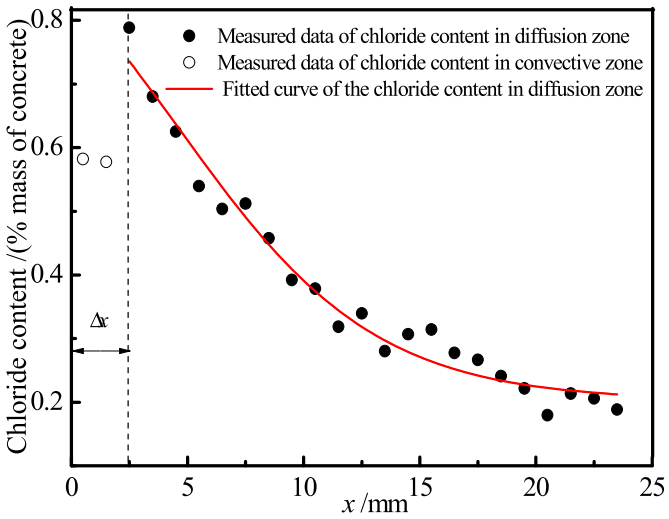

Fig. 13. Chloride concentration distribution in concrete of trestle.

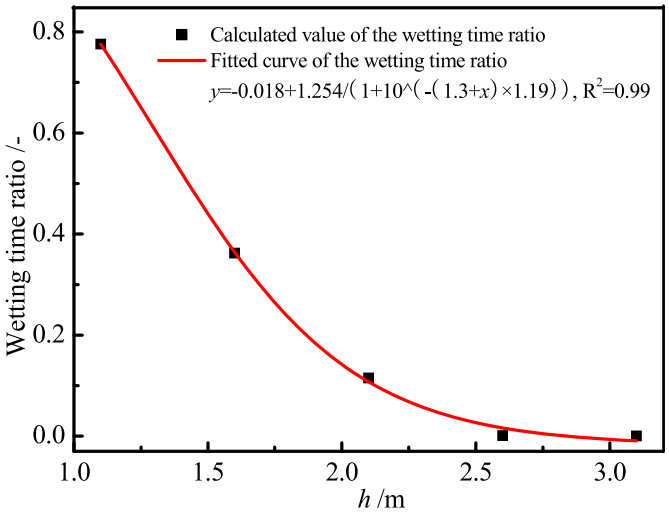

Fig. 14. Curve of wetting time ratio versus elevation.

is approximately 2.5 mm, and the corresponding theoretical calculation result using Eq. (5) is approximately 3.5 mm. Therefore, the chloride convection zone depth model proposed in this study is suitable for predicting the convection zone depth. The equivalent chloride concentration of external environment on concrete surface C_e is approximately 0.63%.

Based on the computational method of the wetting time ratio suggested in Ref. [36] and the data from China maritime service net in Refs. [15], the wetting time ratios for different positions of concrete in-situ environment with time are listed in Table 2. Fig. 14 presents the corresponding variation of the wetting time ratio with elevation.

Table 2 and Fig. 14 illustrate that the wetting time ratio of concrete decreases with increasing elevation and tends to be zero when the elevation is beyond a threshold value. Table 2 also demonstrates that the wetting time ratio differs every month due to the influence of the ocean tide characteristic on the tidal height. Fig. 14 also depicts that the wetting time ratio of concrete varying with elevation can be described by the DoseResp function curve of the Sigmoidal model, providing a novel method for determining the wetting time ratio of RC structures in marine environment.

5. Conclusions

An accurate estimation of the chloride convection zone depth in concrete is significantly important to Fick's second law of diffusion in the life-cycle prediction of RC structures. In this study, a model to estimate the depth of chloride convection zone in concrete was proposed based on the linear variation hypothesis of chloride concentration and water influential depth in convective zone. The results showed that the chloride convection zone depth in concrete was not constant but depended on a function of water influential depth.

Good correlations were found among the surface chloride concentration, elevation and linear distance from the seaside. This correlation can be represented by the S-curve. In addition, chloride diffusion coefficients changed with elevation at different test positions, and the variation followed Gauss distribution. Moreover, the surface chloride concentration increased with increasing time and tends to be constant. The measured data agreed well with the fitted curve, and the modified exponential function fitted to illustrate the change law of chloride concentration with time.

Acknowledgements

This research was supported by the National Natural Science Foundation of China (Nos.51408614, 51422814, U1434204 and 51278496) and Project of Innovation-driven Plan in Central South University (No. 2015CXS014).

References

[1] K. Hong, R.D. Hooton, Effects of cyclic chloride exposure on penetration of concrete cover, Cem. Concr. Res. 29 (1999) 1379–1386.
[2] T. Vidal, A. Castel, R. Francois, Corrosion process and structural performance of a 17 year old reinforced concrete beam stored in chloride environment, Cem. Concr. Res. 37 (2007) 1551–1561.
[3] J.Y. Zhang, Z. Lounis, Sensitivity analysis of simplified diffusion based corrosion initiation model of concrete structures exposed to chlorides, Cem. Concr. Res. 36 (2006) 1312–1323.
[4] O.A. Hodhod, H.I. Ahmed, Modeling the service life of slag concrete exposed to chlorides, J. Ain Shams Eng. 5 (2014) 49–54.
[5] NT Bulid 443, Nordtest method, concrete, hardened: accelerated chloride penetration, Nord. Method 443 (1995).
[6] M. Ismail, A. Toumi, R. Francois, R. Gagne, Effect of crack opening on the local diffusion of chloride in cracked mortar samples, Cem. Concr. Res. 38 (2008) 1106–1111.

[7] C. Andrade, J.M. Diez, C. Alonso, Mathematical modeling of a concrete surface "skin effect" on diffusion in chloride contaminated media, Adv. Cem. Based Mater. 6 (1997) 39–44.
[8] Dura Crete, General Guidelines for Durability Design and Redesign, European Union-Brite Euram III, 2000.
[9] O.T. Rincon, P. Castro, E.I. Moreno, A.A.T. Acosta, O.M. Bravo, I. Arrieta, C. Garcia, D. Garcia, M.M. Madrid, Chloride profiles in two marine structures meaning and some predictions, Build. Envrion. 39 (2004) 1065–1070.
[10] H.L. Ye, N.G. Jin, X.Y. Jin, C.Q. Fu, Model of chloride penetration into cracked concrete subject to drying-wetting cycles, Constr. Build. Mater. 36 (2012) 259–269.
[11] M.F. Lei, L.M. Peng, C.H. Shi, An experimental study on durability of shield segments under load and chloride environment coupling effect, Tunn. Undergr. Sp. Tech. 42 (2014) 15–24.
[12] Z.W. Cui, C.H. Lu, S.F. Zhang, R.G. Liu, Influence of the fly ash content on chloride penetration in flexural cracked concrete, in: 3 rd International Conference on the Durability of Concrete Structures, Queen's University Belfast, 2012.
[13] K.F. Li, C.Q. Li, Z.Y. Chen, Influential depth of moisture transport in concrete subject to drying-wetting cycles, Cem. Concr. Compos. 31 (2009) 693–698.
[14] P. Castro, O.T.D. Rincon, E.J. Pazini, Interpretation of chloride profiles from concrete exposed to tropical marine environments, Cem. Concr. Res. 31 (2001) 529–537.
[15] P. Liu, Research on Similarity of the Chloride Ingress in Concrete under Natural and Artificial Simulation Environment, PhD thesis, Central South University, Changsha, 2013.
[16] J. Crank, The Mathematics of Diffusion, Clarendon Press, Oxford, 1954.
[17] T.U. Mohammed, H. Hamada, Relationship between free chloride and total chloride contents in concrete, Cem. Concr. Res. 33 (2003) 1487–1490.
[18] A.E. Bastidas, A. Chateauneuf, S.M. Sanchez, P. Bressolette, F. Schoefs, A comprehensive probabilistic model of chloride ingress in unsaturated concrete, Eng. Struct. 33 (2011) 720–730.
[19] D. Lockington, J. Parlange, P. Dux, Sorptivity and the estimation of water penetration into unsaturated concrete, Mater. Struct. 32 (1999) 342–347.
[20] Comite Euro-International du Beton, CEB-FIP Model Code 1990: Design Code, Thomas Telford, London, 1993.
[21] P. Aruz, Time dependent models of apparent diffusion coefficient and surface chloride for chloride transport in fly ash concrete, Constr. Build. Mater. 38 (2013) 497–507.
[22] W. Chalee, C. Jaturapitakkul, P. Chindaprasirt, Predicting the chloride penetration of fly ash concrete in seawater, Mar. Struct. 22 (2009) 341–353.
[23] D.A.T. Michael, B.B. Phil, Modelling chloride diffusion concrete: effect of fly ash and slag, Cem. Concr. Res. 29 (1999) 487–495.
[24] F. Duprat, Reliability of RC beams under chloride ingress, Constr. Build. Mater. 21 (2007) 1605–1616.
[25] D.V. Val, P.A. Trapper, Probabilistic evaluation of initiation time of chloride induced corrosion, Reliab Eng. Syst. Safe 93 (2008) 364–372.
[26] H.W. Song, S.W. Pack, K.Y. Ann, Probabilistic assessment to predict the time to corrosion of steel in reinforced concrete tunnel box exposed to sea water, Constr. Build. Mater. 23 (2009) 3270–3278.
[27] K.A. Anders, B.P. Bergsma, C.M. Hansson, Chloride concentration in the pore solution of portland cement paste and portland cement concrete, Cem. Concr. Res. 63 (2014) 35–37.
[28] K.Y. Ann, J.H. Ahn, J.S. Ryou, The importance of chloride content at the concrete surface in assessing the time to corrosion of steel in concrete structures, Constr. Build. Mater. 23 (2009) 239–245.
[29] P.B. Bamforth, The derivation of input data for modeling chloride ingress from eight year UK coastal exposure trials, Mag. Concr. Res. 51 (1999) 87–96.
[30] R.E. Weyers, Service life model for concrete structures in chloride laden environment, J. ACI Mater. 95 (1998) 445–453.
[31] L.P. Tang, Chloride Transport in Concrete Measurement and Prediction, PhD thesis, Chalmers University of Technology, Gotenborg, 1996.
[32] H.W. Song, C.H. Lee, K.Y. Ann, Factors influencing chloride transport in concrete structures exposed to marine environments, Cem. Concr. Compos. 30 (2008) 113–121.
[33] S.W. Pack, M.S. Jung, H.W. Song, S.H. Kim, K.Y. Ann, Prediction of time dependent chloride transport in concrete structures exposed to a marine environment, Cem. Concr. Res. 40 (2010) 302–312.
[34] M.K. Kassir, M. Ghosn, Chloride induced corrosion of reinforced concrete bridge decks, Cem. Concr. Res. 32 (2002) 139–143.
[35] T. Ishida, K. Maekawa, T. Kishi, Enhanced modeling of moisture equilibrium and transport in cementitious materials under arbitrary temperature and relative humidity history, Cem. Concr. Res. 37 (2007) 565–578.
[36] C.J. Yao, Penetration Laws of Chloride Ions in Concrete Infrastructures at Coastal Ports, PhD thesis, Zhejiang University, Ningbo, 2007.